

## Quench sensitivity of 6351 aluminum alloy

Shen-lan LI<sup>1,2</sup>, Zhi-qi HUANG<sup>2,3</sup>, Wei-ping CHEN<sup>1</sup>, Zhi-ming LIU<sup>2</sup>, Wen-jun QI<sup>4</sup>

1. School of Mechanical and Automotive Engineering, South China University of Technology, Guangzhou 510640, China;

2. Guangdong Fenglu Aluminum Co., Ltd., Foshan 528133, China;

3. School of Materials Science and Engineering, Central South University, Changsha 410083, China;

4. Guangzhou Research Institute of Nonferrous Metals, Guangzhou 510650, China

Received 9 July 2012; accepted 7 October 2012

**Abstract:** The quench sensitivity of 6351 alloy was determined by the time–temperature–transformation (TTT) curves and time–temperature–property (TTP) curves by an interrupted quench technique with measurement of as-aged hardness and as-quenched electro-conductivity. The microstructure transformation during isothermal treatment was studied by the transmission electron microscopy (TEM) and Avrami equation. The results showed that the electro-conductivity of the 6351 alloy increased and the hardness decreased with prolonging the holding time at a certain isothermal temperature. The TEM observation indicated that the supersaturated solid solution decomposed and needles  $\beta''$  precipitated at the initial stage of isothermal holding. With the prolongation of holding time at the nose temperature, rod  $\beta'$  and plate  $\beta$  phases formed. The isothermal transformation rate at 360 °C was the fastest, and became slow at 280 °C and reached the slowest at 440 °C. The nose temperatures of the TTT and TTP curves were about 360 °C and the high quench sensitive temperature range was 230–430 °C. The quench factor analysis indicated that the cooling rate should be more than 15 °C/s in the quench sensitive areas in order to get optimal mechanical properties.

**Key words:** 6351 alloy; quench sensitivity; microstructure; cooling rate; quench factor analysis; TTT curve; TTP curve

### 1 Introduction

6xxx Al–Mg–Si alloys are widely used as medium-strength heat-treatable alloys for structural applications due to their excellent formability, weldability and good corrosion resistance. In Al–Mg–Si alloys, Mg and Si are added either in a balanced amount to form binary Al–Mg<sub>2</sub>Si alloys or with excess amount of Si to form the Al–Mg<sub>2</sub>Si quasi-binary composition, to enhance the kinetics of the precipitation process without changing the nature of precipitates [1–3]. Mn addition is generally used to decrease the grain size and restrain recrystallization [4]. In order to achieve optimal mechanical properties, three steps including solution, quenching and aging are generally used in heat-treatable aluminum alloys [5,6]. For alloys with quench sensitivity, quenching is a key step because the mechanical properties strongly depend on the cooling rate during quenching. Inadequate cooling rate often leads to the

drop in strength and hardness after aging. This is attributed primarily to the loss of solute by heterogeneous nucleation and growth of quench precipitates which do not provide strengthening during subsequent aging [7–9]. However, extremely rapid cooling rate will increase the tendency for thin products to distort and thick pieces to develop high levels of residual stress and warping [9]. Consequently, an appropriate quenching rate is necessary in order to minimize the residual stress while maximizing the mechanical properties of the alloy.

At present, there are some different methods to evaluate the quench sensitivity of aluminum alloy, such as end quenching test, temperature–time–transformation (TTT) curve, temperature–time–properties (TTP) curve and continuous-cooling-transformation (CCT) curve [10]. LIU et al [5,6,8] investigated the quench sensitivity of Al–Zn–Mg–Cu alloys by TTP curves including 7055 and 7050 alloys and the influence of quench rate on the drop in the properties was also studied by the quench

factor analysis method. LI et al [7] determined the TTP curve of 7050 aluminum alloy and the microstructure of the alloy under different processes was investigated. They found that the nose temperature and incubation period of the 7050 alloy are about 320 °C and 1.7 s, respectively, and the quench sensitive temperature range is 230–410 °C. ZHANG et al [11] researched the TTP curve of a 7050 alloy by an interrupted quench method and the results show that the quench sensitive temperature range is 240–420 °C with the nose temperature of 330 °C. The TTP curve for 7010 alloy was evaluated by an interrupted quench method into a salt bath and the results indicated that transformation occurs most rapidly between 400 and 250 °C [12]. DOLAN and ROBINSON [13] constructed the TTP diagrams of 7175, 6061 and 2017 aluminum alloys and the critical temperature range of each alloy was identified. However, there is less information available in the published literatures on the TTP and TTT curves of 6xxx series alloys [14–16]. In this work, the quench sensitivity of 6351 aluminum alloy was investigated in order to provide the theoretical foundation for controlling and improving the quench system. The TTT and TTP curves were determined by an interrupted quench method and simulated by Jmatpro software, respectively. The microstructure and phase transformation kinetics during the isothermal treatment were studied by TEM and Avrami equation. The influence of quench rate on the drop in properties was studied by the quench factor analysis method.

## 2 Experimental

The 6351 alloy in this study was supplied in the form of as-extruded sheet with 3 mm in thickness. The chemical composition was Al–1.12Si–0.69Mg–0.5Mn (mass fraction, %). Samples with dimensions of 20 mm (length) × 15 mm (width) × 3 mm (thickness) were prepared. After solution heat treatment at 550 °C for 30 min, the samples were immediately transferred to a salt bath with temperature ranging from 280 °C to 440 °C (step of 20 °C) within 3 s. After isothermal holding for the required duration, the samples were further quenched into cold water at room temperature and then artificially aged at 170 °C for 8 h.

The electro-conductivity tests were made on the as-quenched samples using a D60K metal testing apparatus. Vickers hardness measurement was performed on the aged samples using a WOLPERT 401MVD Vickers hardness testing machines with a load of 9.8 N (1 kg) and holding for 10 s. Five measurements were made for each sample to obtain an average value. The microstructures were examined with a transmission electron microscope (TEM), TECNAIG<sup>2</sup> 20, and an

accelerating voltage of 200 kV was used. The TEM specimens were prepared by cutting a thin slice (about 0.3 mm) from the samples, subsequently punching them to 0.3 mm-diameter discs and by mechanically grinding to thickness around 80 μm, then electro-polishing with a twin-jet polisher in a solution of 30% HNO<sub>3</sub> and 70% CH<sub>3</sub>OH at –25 °C with an applied voltage of 15–20 V.

## 3 Results and discussion

### 3.1 Electro-conductivity and hardness measurement

Figure 1 shows the influence of isothermal treatment on the electro-conductivity and hardness of the investigated alloy. The Vickers hardness of the as-aged sample is HV125 and the conductivity of the as-quenched alloy is 41.7% (vs IACS). From Fig. 1, it can be seen that at a certain temperature, prolonging the isothermal holding time resulted in a reduced hardness and increased conductivity. The electro-conductivity and hardness varied rapidly at the initial stage of isothermal holding and then almost maintained stable. The changing rate was depended on the isothermal holding temperature. At the moderate temperature, such as 340–380 °C, the electro-conductivity increased and the hardness dropped quickly while at higher and lower temperature, the

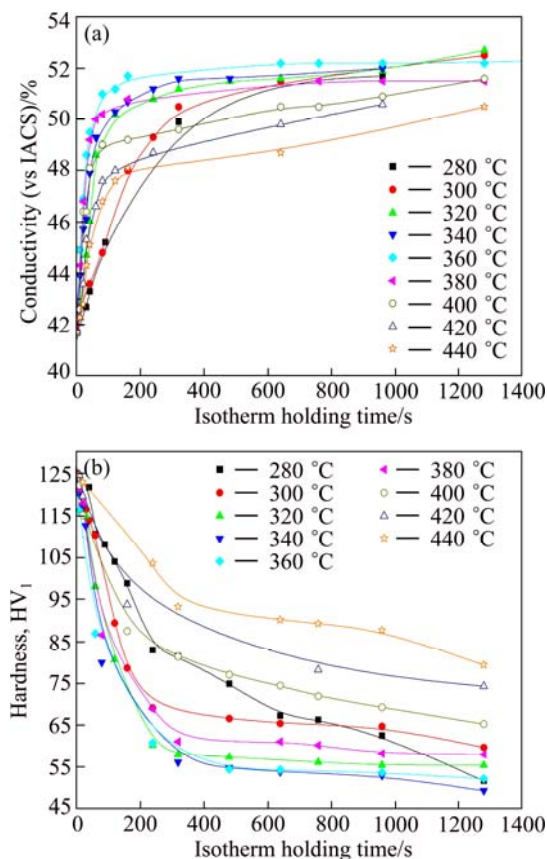


**Fig. 1** Effect of isothermal treatment on electro-conductivity and hardness of 6351 alloy: (a) Electro-conductivity of as-quenched sample; (b) Hardness of as-aged sample

electro-conductivity rose and the hardness declined in a much slower rate with time prolonging. At 360 °C, the properties varied extremely rapidly. About 10% of the maximum hardness was decreased after holding for only 10 s, and further decline can be observed with prolonging isothermal holding time. After 120 s, the hardness decreased almost 50%. The change of hardness and electro-conductivity indicated that some phase transformation should have occurred during the isothermal holding.

### 3.2 TEM microstructure observation

Figure 2 shows a series of TEM bright field images

and selected area electron diffraction (SAED) patterns obtained from the investigated alloy after holding for different time at 360 °C and then artificial aging at 170 °C for 8 h. From Fig. 2(a), it can be seen that after peak aging treatment there are a lot of fine needle shaped metastable precipitates with the size of 20–50 nm in the Al matrix. The needle shaped precipitates homogeneously distributed throughout the matrix. The strain field contrast can be clearly observed around the needle precipitates, which demonstrated that these precipitates are coherent with the matrix. The selected area diffraction pattern (Fig. 2(b)) shows faint cross-shaped diffraction streaks due to the needlelike

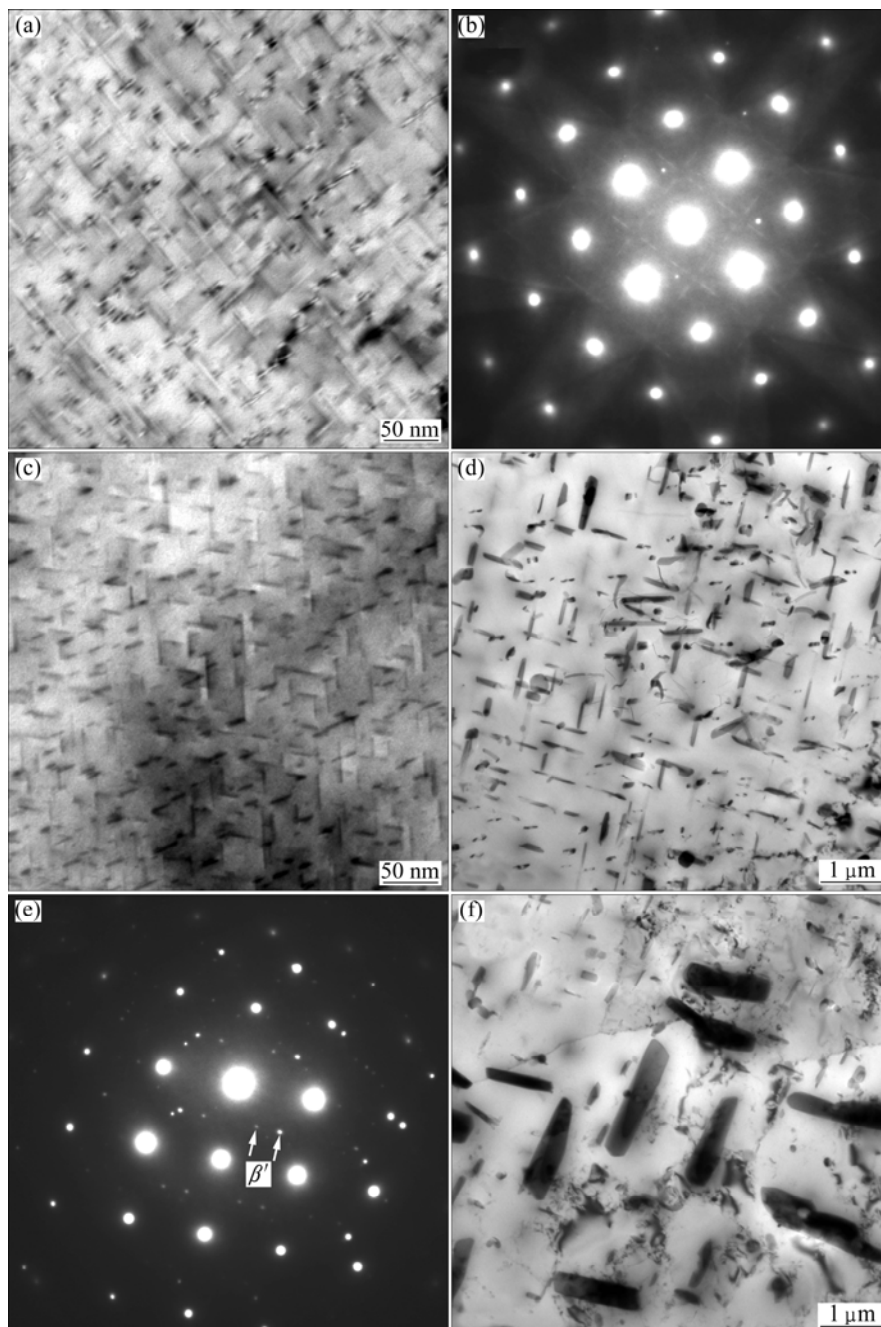


**Fig. 2** TEM images and SAED patterns of 6351 alloy after holding at 360 °C for different time: (a), (b) 0 s; (c) 10 s; (d), (e) 120 s; (f) 1280 s

precipitates. This indicates that the needle-like precipitates should be designated as  $\beta''$  phase. When the holding time is extended to 10 s, the main precipitate is also  $\beta''$  phase, but the length of the needles increased as given in Fig. 2(c). After 120 s isothermal treatment (Fig. 2(d)), most of the needlelike metastable  $\beta''$  phase disappeared and a mass of rod like precipitates with the size of 0.1–1  $\mu\text{m}$  were observed. Some  $\beta'$  variants were observed in the diffraction pattern (Fig. 2(e)). Therefore, it is believed that the rod-like precipitates are  $\beta'$  phase. In the 1280 s isothermal treated specimen, the rod-shaped particles grew up and formed the coarse plate-like  $\beta$  phases, as shown in Fig. 2(f).

The precipitation sequence of 6xxx alloys during aging is generally given as follows [17]: supersaturated solid solution ( $\alpha_{\text{SSS}}$ )  $\rightarrow$  spherical GP zones  $\rightarrow$  needle-like metastable  $\beta''$  phase  $\rightarrow$  rod-like  $\beta'$  phase  $\rightarrow$  platelets of equilibrium  $\beta$  phase. According to the TEM analysis, it can be seen that the precipitation sequence during the isothermal holding process was similar to that during aging. The properties are determined by the precipitate type, density and size. The most effective hardening phase for Al–Mg–Si alloy is  $\beta''$  [18]. The peak aging is associated with a dense population of coherent needle-shaped  $\beta''$  phases, which appear to be optimal barriers for dislocations since they are sheared or cut by glide dislocations. As the isothermal holding continues, the  $\beta''$  phase is reverted to larger and semi-coherent rod-like  $\beta'$  particle. At the final isothermal holding stage, the equilibrium non-coherent  $\beta$  ( $\text{Mg}_2\text{Si}$ ) phases are precipitated. Under this condition, the precipitates are largely bypassed by dislocations through the Orowan mechanism since the precipitates lose coherency. The decrease of hardness with increasing the isothermal holding time is due to the forming of  $\beta'$  and  $\beta$  phases which have little hardening effect and give rise to depletion of Mg and Si solutes in the solid solution.

### 3.3 TTT curves of 6351 alloy

TTT curves of the 6351 alloy obtained by solution-isothermal holding-electro-conductivity measurement method are shown in Fig. 3(a). It can be seen that the TTT curves are “C” shape, and the nose temperature is about 360 °C. The incubation period is very short at the tip of the nose temperature while that is much longer in the lower or higher temperature zone.

The TTT curves simulated by JMatpro 5.1 are shown in Fig. 3(b). It can be seen that the nose temperatures of  $\beta'$  and  $\beta$  precipitations is about 360 °C, while that of the  $\beta$  phase is about 450 °C. It should be noted that the TTT curves created by JmatPro5.1 software distinguished the effects of  $\beta'$ ,  $\beta$  and  $\beta$  phases on the properties while that obtained by experiments can not distinguish the influence of different phases on the

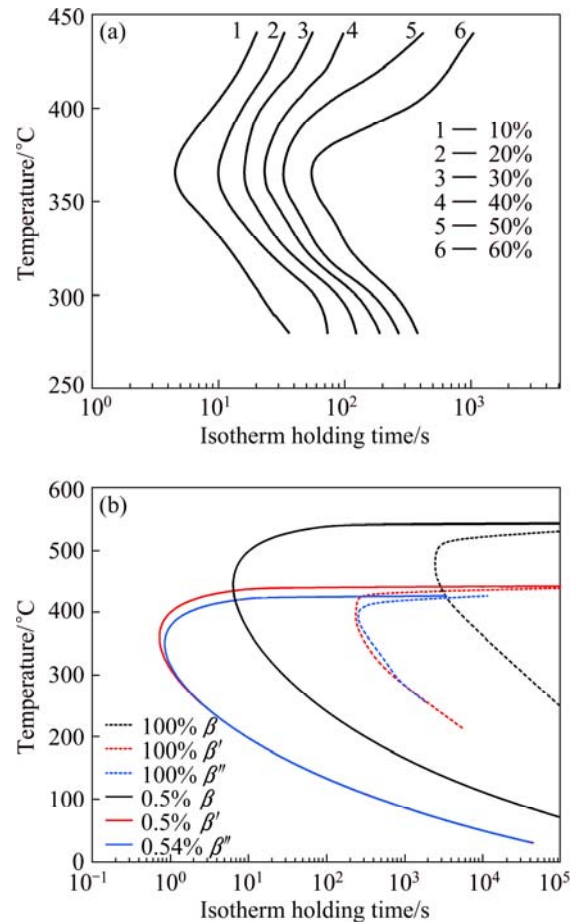


**Fig. 3** TTT curves of 6351 alloy: (a) Experiment; (b) Simulation by JMatPro 5.1 software

electro-conductivity. However, the time for the investigated alloy to finish 60% of its maximum transformation at 360 °C is only about 50 s according to the TTT curves obtained by experiment. The TEM study indicated that the main precipitation is  $\beta'$  phase after 120 s of isothermal treatment at 360 °C. Hence, the above results indicated that the TTT curves measured by experiment are mainly influenced by the  $\beta''$  and  $\beta$  phases.

The kinetics of the isothermal phase transformation is well described by the Johnson–Mehl–Avrami equation [19,20]:  $\zeta = 1 - \exp(-kt^n)$ , where  $\zeta$  is the volume fraction transformed at time  $t$ ,  $k$  is the Avrami constant that depends on the nucleation and the growth rate, very sensitive to temperature and  $n$  is the Avrami exponent which is dependent on the nucleation mechanism. The Avrami parameters  $k$  values are shown in Fig. 4. It has been confirmed that rapid transformations are associated with large  $k$ , i.e., rapid nucleation and growth rates [20]. It can be seen that the  $k$  increased with the isothermal holding temperature decreased and passed through a maximum at 360 °C, as shown in Fig. 4. It is indicated that the phase transformation rate at 360 °C is the fastest, while slower at higher or lower temperature.

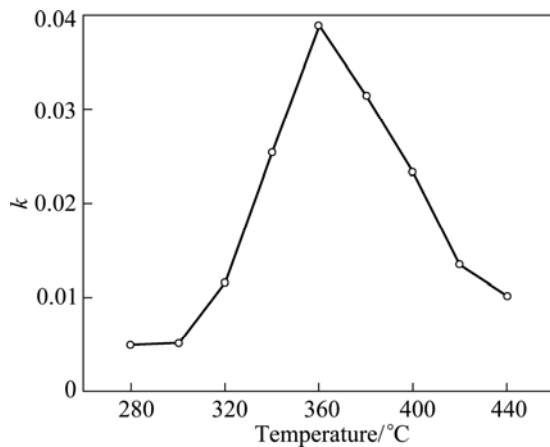


Fig. 4  $k$  value obtained by Johnson–Mehl–Avrami equation fitted at different temperatures

### 3.4 TTP curves of 6351 alloy

TTP curves can be described by an equation [21]:

$$C(T) = -k_1 k_2 \exp\left(\frac{k_3 k_4^2}{RT(k_4 - T)^2}\right) \exp\left(\frac{k_5}{RT}\right) \quad (1)$$

where  $C(T)$  is the critical time required to precipitate a constant amount of solute;  $k_1$  is the constant which equals the natural logarithm of the fraction untransformed during quenching;  $k_2$  is the constant related to the reciprocal of the number of nucleation sites;  $k_3$  is the constant related to the energy required to form a nucleus;  $k_4$  is the constant related to the solvus temperature;  $k_5$  is the constant related to the activation energy for diffusion;  $R$  is the mole gas constant;  $T$  is the thermodynamic temperature.

According to the hardness data for the investigated alloy, the coefficients  $k_2$ – $k_5$  in Eq. (1) can be determined as listed in Table 1. With the data in Table 1 and Eq. (1), the TTP (Vickers hardness) curves for the 6351 alloy plotted at 99.5%, 95%, 90%, 80% and 70% of the maximum property may be constructed as shown in Fig. 5. It is clearly shown that there is a good agreement between experimental data and the fitted TTP curves, and the nose temperature is about 360 °C. According to the location of the TTP curve of 99.5% of the highest property shown in Fig. 5, when the transformation time is 10 s, the high quench sensitivity temperature zone is 230–430 °C. In this zone, the incubation period is short and time spent in this region must be minimized during the quenching so that high mechanical properties can be achieved.

Table 1  $k_2$ – $k_5$  coefficients of TTP curves for 6351 aluminum alloy by fitting

$k_2/s$	$k_3/(J \cdot mol^{-1})$	$k_4/K$	$k_5/(J \cdot mol^{-1})$
$4.0417 \times 10^{-12}$	7753	1008	111812

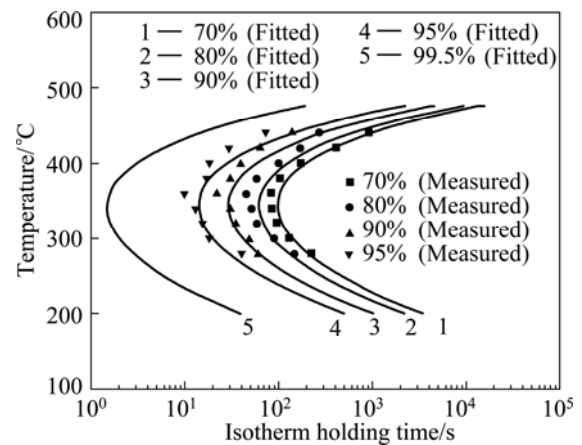


Fig. 5 TTP curves of 6351 aluminum alloy

Aluminum quenching is based on the nucleation theory and the precipitation process of supersaturated solid solution is diffusion controlled reaction [6,11]. At high temperatures close to solution heat treatment temperature, nucleation rates are small because of the low degree of supersaturation, and so the precipitation rates are low despite the high diffusion rates. Therefore, it takes a considerable amount of time for precipitations to occur because the driving force for transformation is very small due to the small undercooling. At lower temperatures, the diffusion rate is low, and thus the precipitation rate is low despite the high degree of supersaturation. So the time required for precipitation increases again. At intermediate temperatures, the precipitation rate is the highest because of the large driving force and high diffusion rate of solute atoms [7,13,21,22]. Consequently, the precipitation rate is the fastest in a critical temperature range. For the 6351 alloy in this study, the nose temperature of the TTP curves is about 360 °C and the critical temperature range is 230–430 °C. Therefore, to prevent premature precipitation, it is necessary to quench the alloys at very rapid rates through the critical temperature. The incubation period reflected the stability of supersaturated solid solution, and the longer the incubation period, the more stable the supersaturated solid solution. From the TTP curves shown in Fig. 5, it can be seen that the incubation period is the shortest, near the nose temperature. In this zone, the supersaturated solid solution is the most unstable, the precipitate rate is fastest and the quench sensitivity is the highest.

### 3.5 Quench factor analysis

With the TTP curves, the effect of quench rate on the properties can be predicted by the quench factor analysis method. The relationships between the mechanical property and the quench factor can be pressed as:  $\sigma = \sigma_{\max} \exp(k_1 \tau)$  [13,23], where  $\tau$  is the quench

factor,  $\sigma_{\max}$  is the maximum property that can be attained after a fast quenching and  $\sigma$  is the predicted value. In this work, the time step interval  $\Delta t=0.2\text{s}$  is used and  $k_1=\ln(0.995)$ . The influence of average quench rates of 0.5–100 °C/s through the high quench sensitivity temperature range of 230–430 °C was investigated. The relationships between the quench factor  $\tau$  and the predicted hardness and the cooling rate are shown in Fig. 6. It can be seen that low values of quench factor  $\tau$  are associated with high cooling rates, minimum precipitations during cooling and high hardness. During the continuous cooling process, the precipitation of supersaturated solid solution is heterogeneous. When the cooling rate is very slow, the supersaturation is decreased because of the nucleation of the coarse second phase, and thus the age hardening effect is reduced; when the cooling rate is greater than a certain critical value  $Q_c$ , a supersaturated solid solution is retained since the precipitation can be suppressed and there is not enough time for the second phase to nucleate and grow up. According to Fig. 6, the hardness of the 6351 alloy reaches more than 97% of the maximum property when the cooling rate is about 15 °C/s while the hardness increases slowly when the cooling rate is higher than 15 °C/s. Therefore, the  $Q_c$  is estimated as about 15 °C/s for the 6351 alloy. In the high quench sensitivity temperature range of 230–430 °C, where the cooling rate has a significant impact on the mechanical properties of the alloy, the cooling rate should be high (more than 15 °C/s) to ensure that a supersaturated solid solution is retained, while at higher or lower temperature, decreasing the cooling rate is helpful to relieve the effect of residual stress.

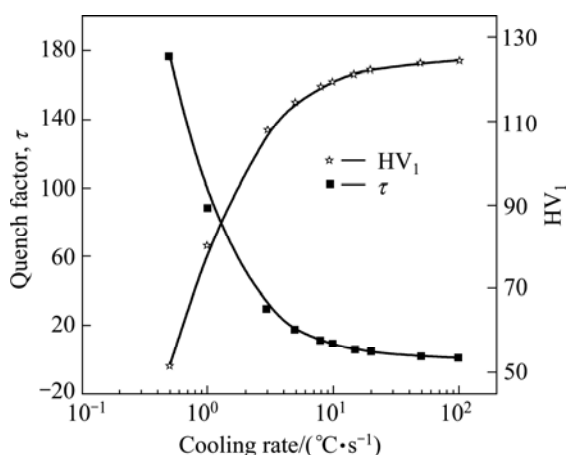


**Fig. 6** Effect of average cooling rate on quench factor and predicted hardness of 6351 alloy

CCT curves obtained from simulation in Fig. 7 show that, the critical cooling rate of the 6351 alloy without  $\beta'$  and  $\beta$  phase precipitations is about 13 °C/s, which further confirms the results predicted by the

quench factor analysis while the critical cooling rate calculated by quench factor analysis is estimated to be about 15 °C/s.

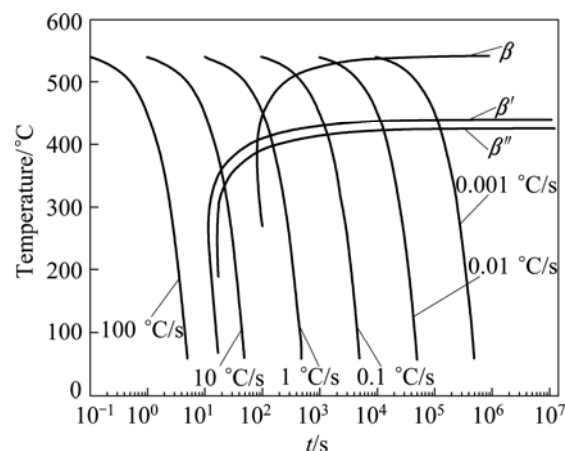


**Fig. 7** CCT curves of 6351 aluminum alloy simulated by JMatPro 5.1 software

## 4 Conclusions

1) The nose temperatures of the TTP and TTT curves of the 6351 alloy are about 360 °C and the high quench sensitivity temperature zone is 230–430 °C.

2) The isothermal transformation rate at 360 °C is the fastest, and becomes slow at higher or lower temperature.

3) According to the prediction by the quench factor analysis, in order to get optimal mechanical properties, the alloy should be first slowly cooled from the solution heat treatment temperature to the temperatures above the critical temperature region and then fast cooled at more than 15 °C/s in the high quench sensitivity temperature range of 230–430 °C.

## References

- [1] MURAYAMA M, HONO K, MIAO W F, LAUGHLIN D E. The effect of Cu additions on the precipitation kinetics in an Al–Mg–Si alloy with excess Si [J]. *Metallurgical and Materials Transactions A*, 2001, 32: 239–246.
- [2] ZHEN L, FEI W D, KANG S B, KIM H W. Precipitation behaviour of Al–Mg–Si alloys with high silicon content [J]. *Journal of Materials Science*, 1997, 32: 1895–1902.
- [3] LYNCH J P, BROWN L M, JACOBS M H. Microanalysis of age-hardening precipitates in aluminium alloys [J]. *Acta Metallurgica*, 1982, 30: 1389–1395.
- [4] YUCEL B. The effect of processing and Mn content on the T5 and T6 properties of AA6082 profiles [J]. *Journal of Materials Processing Technology*, 2006, 173: 84–91.
- [5] LIU S D, ZHONG Q M, ZHANG Y, LIU W J, ZHANG X M, DENG Y L. Investigation of quench sensitivity of high strength Al–Zn–Mg–Cu alloys by time–temperature–properties diagrams [J]. *Materials and Design*, 2010, 31: 3116–3120.
- [6] LIU Sheng-dan, ZHANG Xin-min, YOU Jiang-hai, HUANG Zhen-bao, ZHANG Chong, ZHANG Xiao-yan. TTP curves of 7055

- aluminum alloy and its application [J]. The Chinese Journal of Nonferrous Metals, 2006, 16(12): 2034–2039. (in Chinese)
- [7] LI Pei-yua, XIONG Bai-qing, ZHANG Yong-an, LI Zhi-hui, ZHU Bao-hong, WANG Feng, LIU Hong-wei. Hardenability characteristic and microstructure of 7050 Al alloy [J]. The Chinese Journal of Nonferrous Metals, 2011, 21(3): 514–521. (in Chinese)
- [8] LIU Sheng-dan, ZHANG Xin-ming, YOU Jiang-hai, ZHANG Xiao-yan. Influence of trace Zr on quench sensitivity of 7055 type aluminum alloy [J]. Rare Metal Materials and Engineering, 2007, 36(4): 607–611. (in Chinese)
- [9] MURAT T, RALPH T S. Quench sensitivity of 2219-T87 aluminum alloy plate [J]. Materials Science and Engineering A, 2010, 527: 5033–5037.
- [10] SHANG Bao-chuan, YIN Zhi-min, HUANG Zhi-qi, ZHOU Xiang. Research methods and status of the hardenability of aluminum alloy [J]. Light Alloy Fabrication Technology, 2010, 38(10): 4–8. (in Chinese)
- [11] ZHANG Xin-ming, LIU Wen-jun, LIU Sheng-dan, YUAN Yu-bao, DENG Yun-lai. TTP curve of aluminum alloy 7050 [J]. The Chinese Journal of Nonferrous Metals, 2009, 19(5): 861–868. (in Chinese)
- [12] ROBINSON J S, CUDD R L, TANNER D A, DOLAN G P. Quench sensitivity and tensile property inhomogeneity in 7010 forgings [J]. Journal of Materials Processing Technology, 2001, 119: 261–267.
- [13] DOLAN G P, ROBINSON J S. Residual stress reduction in 7175-T73, 6061-T6 and 2017-T4 aluminium alloys using quench factor analysis [J]. Journal of Materials Processing Technology, 2004, 153–154: 346–351.
- [14] SHANG B C, YIN Z M, WANG G, LIU B, HUANG Z Q. Investigation of quench sensitivity and transformation kinetics during isothermal treatment in 6082 aluminum alloy [J]. Materials and Design, 2011, 32: 3818–3822.
- [15] XIAO Cong-wen, WANG Ming-pu, WANG Zheng-an, LI Zhou, GUO Ming-xing. Quench sensitivity of 6005A aluminum alloy [J]. The Chinese Journal of Nonferrous Metals, 2003, 13(3): 635–639. (in Chinese)
- [16] YAN Si, YIN Zhi-min, HUANG Zhi-qi, SHANG Bao-chuan. Isothermal transformation of 6061 aluminum alloy and its application of TTP curves [C]//Proceedings of LW 2010 the 4th Aluminum Profile Technology Seminar. Guangzhou, 357–361. (in Chinese)
- [17] MAISONNETTE D, SUERY M, NELIAS D, CHAUDET P, EPICIER T. Effects of heat treatments on the microstructure and mechanical properties of a 6061 aluminium alloy [J]. Materials Science and Engineering A, 2011, 528: 2718–2724.
- [18] GRAZYNA M N, JAN S. Influence of heat treatment on the microstructure and mechanical properties of 6005 and 6082 aluminium alloys [J]. Journal of Materials Processing Technology, 2005, 162–163: 367–372.
- [19] XIAO Ji-mei. The alloy phase and phase transformation [M]. Beijing: Metallurgical Technology Press, 2004: 310–312. (in Chinese)
- [20] PORTER D A, EASTERLING K E. Phase transformations in metals and alloys [M]. London: Chapman & Hall Press, 1992: 263–381.
- [21] XIONG Bai-qing, LI Xi-wu, ZHANG Yong-an, LI Zhi-hui, ZHU Ba-hong, WANG Feng, LIU Hong-wei. Quench sensitivity of Al–Zn–Mg–Cu alloys [J]. The Chinese Journal of Nonferrous Metals, 2011, 21(10): 2631–2638. (in Chinese)
- [22] LIU Sheng-dan, ZHANG Xin-ming, HUANG Zhen-bao, LIU Wen-hui, YOU Jiang-hai. Quench sensitivity of 7055 aluminum alloy [J]. Journal of Central South University: Science and Technology, 2006, 37(5): 846–849. (in Chinese)
- [23] DOLAN G P, FLYNN R J, TANNER D A, ROBINSON J S. Quench factor analysis of aluminium alloys using the Jominy end quench technique [J]. Materials Science and Technology, 2005, 21: 687–692.

## 6351 铝合金的淬火敏感性

李慎兰<sup>1,2</sup>, 黄志其<sup>2,3</sup>, 陈维平<sup>1</sup>, 刘志铭<sup>2</sup>, 戚文军<sup>4</sup>

1. 华南理工大学 机械与汽车工程学院, 广州 510640;
2. 广东凤铝铝业有限公司, 佛山 528133;
3. 中南大学 材料科学与工程学院, 长沙 410083;
4. 广州有色金属研究院, 广州 510650

**摘要:** 采用分级淬火的实验方法, 结合合金时效态硬度和淬火态电导率的测试拟合得到 6351 合金的 TTP 和 TTT 曲线, 并采用透射电镜对 6351 合金的淬火敏感性进行研究。结果表明, 当 6351 合金在相同温度下等温时, 随着保温时间延长, 淬火态电导率呈上升趋势, 时效态硬度呈下降趋势。透射电镜分析发现, 在等温初期, 过饱和固溶体分解形成针状的  $\beta''$  相; 随着保温时间延长, 逐渐形成棒状  $\beta'$  相和片状  $\beta$  相。TTT 和 TTP 曲线的鼻温为 360 °C, 淬火敏感温度区间为 230–430 °C。在鼻温附近等温相转变最快, 低温区相转变次之, 高温区最慢。淬火因子分析结果表明, 要获得最佳的力学性能, 淬火敏感温度区间的冷却速率需大于 15 °C/s。

**关键词:** 6351 合金; 淬火敏感性; 组织结构; 冷却速率; 淬火因子分析; TTT 曲线; TTP 曲线

(Edited by Hua YANG)